

Effects of shear keys on seismic performance of an isolation system

Biao Wei^{*1,2}, Chaobin Li^{1,2a}, Xiaolong Jia^{1,2b}, Xuhui He^{1,2c} and Menggang Yang^{1,2d}

¹School of Civil Engineering, Central South University, 22 Shaoshan South Road, Changsha, China

²National Engineering Laboratory for High Speed Railway Construction,
22 Shaoshan South Road, Changsha, China

(Received January 12, 2019, Revised April 19, 2019, Accepted April 26, 2019)

Abstract. The shear keys are set in a seismic isolation system to resist the long-term service loadings, and are cut off to isolate the earthquakes. This paper investigated the influence of shear keys on the seismic performance of a vertical spring-viscous damper-concave Coulomb friction isolation system by an incremental dynamic analysis (IDA) and a performance-based assessment. Results show that the cutting off process of shear keys should be simulated in a numerical analysis to accurately predict the seismic responses of isolation system. Ignoring the cutting off process of shear keys usually leads to untrue seismic responses in a numerical analysis, and many of them are unsafe for the design of isolated structure. And those errors will be increased by increasing the cutting off force of shear keys and decreasing the spring constant of shear keys, especially under a feeble earthquake. The viscous damping action postpones the cutting off time of shear keys during earthquakes, and reduces the seismic isolation efficiency. However, this point can be improved by increasing the spring constant of shear keys.

Keywords: seismic isolation; shear key; friction; viscous damper; spring

1. Introduction

Some friction devices were invented to achieve a more optimum seismic isolation performance than that of the traditional isolation devices (Ismail *et al.* 2015, Siringoringo and Fujino 2015). Harvey and Gavin (2013) investigated a rolling friction platform formed by four pairs of recessed steel bowls to isolate objects under horizontal earthquakes, and found that a uni-axial model was not able to predict those seismic responses. Harvey, Wiebe and Gavin (2013) also found that very chaotic behavior including impacts happened for a similar rolling-pendulum during earthquakes. Harvey and Gavin (2014) identified that the little change of initial conditions would influence the seismic isolation performance when carrying out the numerical analysis and test of double rolling isolation systems (RISs). Based on the above influence factors, a simplified mathematical model was presented to successfully predict the maximum seismic response values by Harvey *et al.* (2014). Furthermore, a new mathematical model with more reduced order was proposed to calculate the seismic responses of RISs with different damping

components by Harvey and Gavin (2015). Ismail and Casas (2014) validated that a roll-n-cage device was an efficient solution in protecting cable-stayed bridges (Ismail *et al.*, 2014) and other structures (Ismail 2015) against near-fault earthquakes. Wang *et al.* (2014) achieved a perfect in-plane performance isolating earthquakes by using multi sloped friction devices. Ortiz, Magluta and Roitman (2015) used a mathematical model to predict the responses of roller-bearing isolated buildings under earthquakes and validated it using an experiment. As to reduce the structural residual displacement after earthquakes, the elliptical rolling rods (Jangid and Londhe 1998) or spring-rolling devices (Jangid, 2000) were used to support the building structures. Antonyuk and Plakhtienko (2004) joined the rolling and sliding devices together to isolate the building structures. A bearing using self-centering and supplemental energy dissipation friction devices was proposed to isolate the highway bridges under earthquakes (Ou *et al.* 2010, Lee *et al.* 2010). Cui (2012) carried out a concrete, rubber and polyurethane ball tests to support the building floor under earthquakes. Similarly, Luís Guerreiro (2007) performed a rolling ball test to reduce the seismic acceleration response of light structures. Tsai (2010) used an interchange between the steel balls under the long-term service time and the damping balls under the earthquake time to prolong the service time of seismic isolation devices.

Kurita (2011) and Nanda (2012) found that the friction-based isolation devices could reduce the structural acceleration response by 50-90%, and were the optimum devices to isolate the ground motion. However, many of the above researches ignored the influence of shear keys on the seismic isolation efficiency.

Shear keys were always added to the seismic isolation device to resist the long-term service loads, and were cut off

*Corresponding author, Professor

E-mail: weibiao@csu.edu.cn

^a Graduate Research Assistant

E-mail: lichaobin@csu.edu.cn

^b Graduate Research Assistant

E-mail: 184812231@csu.edu.cn

^c Professor

E-mail: xuhuihe@csu.edu.cn

^d Professor

E-mail: mgyang@csu.edu.cn

to isolate the seismic energy under designed earthquakes (Wei *et al.* 2018d). However, many factors would disturb the cutting off of shear keys as follows:

(1) The uneven distribution of friction coefficient in space (Wei *et al.* 2018a, Wang *et al.* 2010, Wei *et al.* 2018b), due to the rough contact surface (Begley and Virgin 1998, Flom and Bueche 1959), could cause uncertain seismic responses (Wei *et al.* 2019b, Yim *et al.* 1980), and the shear keys would be well although they were designed to fail under a certain earthquake.

(2) As to decrease the structural relative and residual displacements of friction-based devices (Kosantiniadis and Makris 2009, Lewis and Murray 1995), the springs or viscous dampers were used to add the restoring or damping forces (Wei *et al.* 2019b). However, Chung *et al.* (2015) and Wei *et al.* (2019b) found that a too much damping or a too strong spring was inappropriate and would increase the structural acceleration response, and the constant spring stiffness would lead to a resonance during earthquakes. On the contrary, if the restoring devices were weak, the friction force would prevent the structure from returning to the initial position and a large residual displacement implied a huge repair cost after earthquakes. Although the shape memory alloy (SMA) devices could solve the above contradiction between the acceleration and displacement responses, they were too expensive to be widely used in the practical engineering (Ozbulut and Hurlbaas 2012, Abdulridha *et al.* 2013).

It is necessary to investigate the details that the above factors, such as the friction action, the spring action and the viscous damping action, disturb the cutting off of shear keys, or how to avoid the disturbing factors and how the shear keys influence the seismic isolation efficiency.

This paper analyzes the influence of shear keys on the structural acceleration and displacement responses of a vertical spring-viscous damper-concave Coulomb friction isolation system under earthquakes. The above isolation system has two merits at least: (1) the degree disturbing the cutting off process of shear keys is weakened, because the horizontal spring and friction forces are the smallest at the initial position; (2) after the cutting off of shear keys during an earthquake, the horizontal spring and friction forces gradually increase to reduce the displacement responses when the isolator moves from the initial position.

2. A vertical spring-viscous damper-concave coulomb friction isolation system

Fig. 1 schematically describes an idealized vertical spring-viscous damper-concave Coulomb friction isolation system with shear keys.

2.1 Structure mass

As to avoid the influence of high order vibration modes on the research topic of this paper, a single-degree-of-freedom structure with a mass M of 300t was set as the isolated structure (Wei *et al.* 2018a).

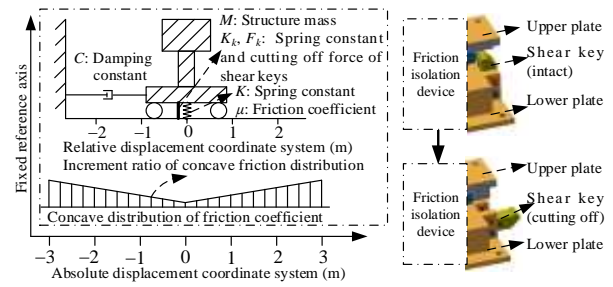


Fig. 1 A vertical spring-viscous damper-concave Coulomb friction isolation system

2.2 Shear keys

The horizontal component of spring force was 0 and the friction force of concave friction contact surface was very small when the structural relative displacement $d_r = 0$. Therefore, shear keys were added to the seismic isolation device to resist the long-term service loads, and were cut off to isolate the seismic energy under designed earthquakes.

The spring constant K_k of shear keys in Fig. 1 adopted 20000, 40000, 60000, 80000 and 100000 kN/m, respectively. As for each spring constant K_k , the cutting off force F_k of shear keys adopted 10, 50, 100, 150 and 200kN, respectively. Finally, there were 25 shear key cases.

2.3 Spring

The spring element remains elastic during earthquakes, and it is able to reduce the relative and residual displacements between the structure and the ground. The spring constant K of vertical spring adopted 100, 200, 300, 400, 500 and 600 kN/m, respectively. The length of spring with zero stress is defined as h_0 while the initial length in Fig. 1 is represented by h_1 . The values of h_1 adopted 0.5 and 1.0 m, respectively. As for the case of $h_1 = 0.5$ m, the values of h_0 respectively adopted 0.1, 0.2, 0.3, 0.4 and 0.5 m, and the ratio h_0/h_1 was respectively 0.2, 0.4, 0.6, 0.8 and 1.0. An increase of ratio implies that the spring becomes looser in the initial condition. In terms of the case of $h_1 = 1.0$ m, the values of h_0 respectively adopted 0.1, 0.2, 0.4, 0.6, 0.8 and 1.0m, and the ratio h_0/h_1 was respectively 0.1, 0.2, 0.4, 0.6, 0.8 and 1.0.

When the structural relative displacement d_r happens, the spring force F_s is

$$F_s = K(\sqrt{h_1^2 + d_r^2} - h_0) \quad (1)$$

The horizontal component F_{sh} and the vertical component F_{sv} of the resultant force of spring and shear keys are respectively

$$F_{sh} = K \left(\sqrt{h_1^2 + d_r^2} - h_0 \right) \frac{d_r}{\sqrt{h_1^2 + d_r^2}} + K_k d_r \quad (2)$$

$$(K_k d_r \leq F_k)$$

$$F_{sh} = K(\sqrt{h_1^2 + d_r^2} - h_0) \frac{d_r}{\sqrt{h_1^2 + d_r^2}} \quad (K_k d_r > F_k) \quad (3)$$

$$F_{sv} = K(\sqrt{h_1^2 + d_r^2} - h_0) \frac{h_1}{\sqrt{h_1^2 + d_r^2}} \quad (4)$$

When the structural relative displacement d_r is 0, F_{sh} is 0. Simultaneously, both of the spring force and its vertical component are $K(h_1 - h_0)$. And those values become 0 if $h_1 = h_0$, which means that the initial condition of spring in Fig. 1 has zero stress.

The horizontal secant constant K_{sh} of spring and shear keys is

$$K_{sh} = K \left(\sqrt{h_1^2 + d_r^2} - h_0 \right) \frac{1}{\sqrt{h_1^2 + d_r^2}} + K_k \quad (5)$$

$$(K_k d_r \leq F_k)$$

$$K_{sh} = K(\sqrt{h_1^2 + d_r^2} - h_0) \frac{1}{\sqrt{h_1^2 + d_r^2}} \quad (K_k d_r > F_k) \quad (6)$$

Eqs. (5) and (6) can also be expressed as

$$K_{sh} = K \left(1 - \frac{1}{\sqrt{\left(\frac{h_1}{h_0}\right)^2 + \left(\frac{d_r}{h_0}\right)^2}} \right) + K_k \quad (K_k d_r \leq F_k) \quad (7)$$

$$K_{sh} = K \left(1 - \frac{1}{\sqrt{\left(\frac{h_1}{h_0}\right)^2 + \left(\frac{d_r}{h_0}\right)^2}} \right) \quad (K_k d_r > F_k) \quad (8)$$

2.4 Viscous damper

The viscous damper can produce a viscous damping force and dissipate earthquake energy during earthquakes. The damping constants C adopted 0, 50, 100, 150, 200 and 250 kN·s/m in this paper.

2.5 Coulomb friction

In this system, the friction device supports the superstructure and isolates the earthquake input motion. During a seismic event, it could induce friction force at the bottom of structure to balance the inertial force developed in the superstructure, and dissipate the earthquake energy. Despite the fact that both the friction device and the viscous damper are the energy dissipation components, the force of friction device is a function of friction coefficient and pressure force while the force of viscous damper is dependent on the damping constant and relative velocity. Furthermore, the friction device prevents the structure from returning to its initial center, however, the viscous damper doesn't have such a negative effect.

As to reduce this negative effect, Fig. 1 adopted a concave distribution of friction coefficient in space. The friction coefficient increased from the central friction coefficient $\mu_0 = 0.005$ to the larger values with an increment ratio R when the structure moved away from the central position under earthquakes. The increment ratio R

was assumed to be 0.01, 0.02, 0.03, 0.04 and 0.1m^{-1} , respectively. Therefore, the horizontal friction force F_{fh} is

$$F_{fh} = (\mu_0 + R d_r) [mg + K(\sqrt{h_1^2 + d_r^2} - h_0) \frac{h_1}{\sqrt{h_1^2 + d_r^2}}] \quad (9)$$

When d_r increases during earthquakes, the friction force increases, due to the concave pattern of friction coefficient and the increased vertical component of spring force, to dissipate the earthquake energy more significantly to avoid a larger relative displacement. Simultaneously, the horizontal component of spring force also increases to reduce the relative and residual displacements. Theoretically, the system in Fig. 1 is reasonable to reduce the structural seismic responses. And it is necessary to carry out the parameter optimization analysis of the system.

3. Ground motion

An elastic response spectrum with Chinese soil type III (JTJ 004-89) and a peak ground acceleration (PGA) of 1 g was selected for the target spectrum as shown in Fig. 2 (Wei *et al.* 2018c). The relatively soft soil with a shear wave velocity between 140 and 250 m/s was assumed very thick for the structural site.

20 ground motions, selected from the Pacific Earthquake Engineering Research Center database (PEER 2015), were listed in Fig. 2. Their PGA were adjusted to make their mean spectrum be close to the target spectrum. And then the above scaled PGA of 20 ground motions were continuously scaled from 0.01 g to 1 g with an increment of 0.01 g, and those ground motions were input into the isolation structure.

4. Calculation method

A computer program was compiled to calculate the seismic responses of the vertical spring-viscous damper-concave Coulomb friction system, and its mathematical foundation was listed in the following content.

As to describe the movement of ground and structure in mathematics, the coordinate system using the absolute displacement is defined in Fig. 1. The seismic response of ground is represented by the symbols a_e , v_e , d_e which represent the absolute acceleration, velocity and displacement of ground. And the symbols a_s , v_s , d_s represent the corresponding absolute responses of structure, respectively.

The relationship between v_e and v_s could lead to 2 different scenarios as follows:

(1) $v_e \neq v_s$. It implies that the structure moves slower or faster than the ground, which produces the structural motion relative to the ground in the coordinate system of Fig. 1. The horizontal force of isolated structure should be the sum of the horizontal forces of spring, friction, shear key and viscous damper which can be expressed as $[\pm F_{fh} + F_{sh} + C(v_e - v_s)]$. The sign of F_{fh} should be positive when $v_e > v_s$ and be negative when $v_e < v_s$.

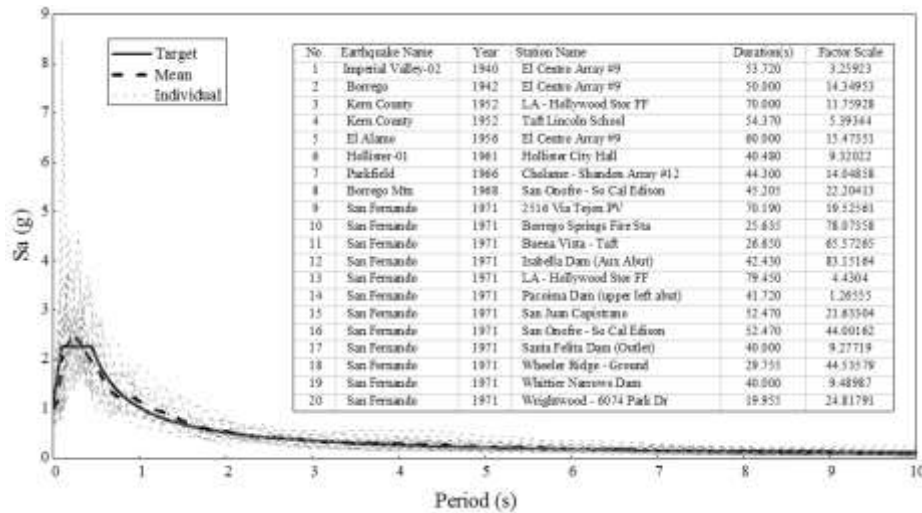


Fig. 2 Target spectrum, mean spectrum and individual earthquake spectra

At a certain time step of case (1), if $|(v_s - v_e) + F_{sh}\Delta t_i/m + C(v_e - v_s)\Delta t_i/m| \leq F_{fh}\Delta t_i/m$ and $|[a_e - F_{sh}/m - C(v_e - v_s)/m]| \leq F_{fh}/m$, the system will move to case (2), i.e., $v_e = v_s$, where $\Delta t_i = t_i - t_{i-1}$ and t_i is the i th time of the ground motion input.

(2) $v_e = v_s$. It implies that the structure moves with the same velocity as the ground. The equation of motion can be expressed as $ma_e = \pm F_{friction} + F_{sh} + C(v_e - v_s)$, where $F_{friction} \leq F_{fh}$. And the equation is further simplified as $ma_e = \pm F_{friction} + F_{sh}$ since $v_e = v_s$, or $|[a_e - F_{sh}/m]| = F_{friction}/m \leq F_{fh}/m$. In order to estimate the structural response at the next time step, it is necessary to compare $|[a_e - F_{sh}/m]|$ with F_{fh}/m :

① when $|[a_e - F_{sh}/m]| \leq F_{fh}/m$, the inertia force developed in the structure is not able to trigger the relative movement between the structure and the ground. Therefore, the structure has the same acceleration as the ground.

② when $|[a_e - F_{sh}/m]| > F_{fh}/m$, the instantaneous ground motion is intense enough to develop the structural new movement relative to the ground. Therefore, the force of isolated structure could be mathematically expressed as $[\pm F_{fh} + F_{sh} + C(v_e - v_s)]$. And the system will move to case (1), i.e. $v_e \neq v_s$, at the next time step.

5. Performance-based assessment process

To evaluate the structural seismic responses and vulnerabilities, the performance-based earthquake engineering (PBEE) method of PEER is simplified to only include the response analysis and the damage analysis.

An incremental dynamic analysis (IDA), using the above ground motion records and the above calculation method, can obtain the structural response distributions under the earthquakes with different PGA. Before the cutting off of shear keys, the natural periods of isolation system are 0.344~0.769s. Temporary resonance trend may happen for the isolation system, when comparing the natural periods with the predominant period 0.45s of ground

motions in Fig. 2. However, the large force, due to the temporary resonance trend, cuts off the shear keys. And then the natural periods of isolation system become much longer than 0.769s, and the temporary resonance trend and large force suddenly disappear. Therefore, the cutting off force of shear keys controls the structural peak acceleration response. After the cutting off of shear keys, the structural displacement responses become much larger.

The damage states (DS) of structural system are defined in Table 1. The structural peak acceleration response reflects the structural inertia force, and is the most important index of seismic isolation efficiency. The structural relative displacement is another index of seismic isolation efficiency, because it determines the size of structural foundation and the gap value from the adjacent structure. The index of structural residual displacement should be paid more attention, because it determines the repair cost after earthquakes.

6. Performance-based assessment results

The combination of 1 structural mass, 6 damping constants, 5 friction cases, 66 spring cases and 25 shear key cases produced 49500 cases. Those cases would be subjected to the earthquakes with different PGA.

Table 1 Damage states of structural systems

Index	DS1	DS2	DS3	DS4
Acceleration (m/s ²)	0.25	0.50	0.75	1.00
Relative Displacement (m)	0.20	0.40	0.80	1.60
Residual Displacement (m)	0.02	0.04	0.08	0.16

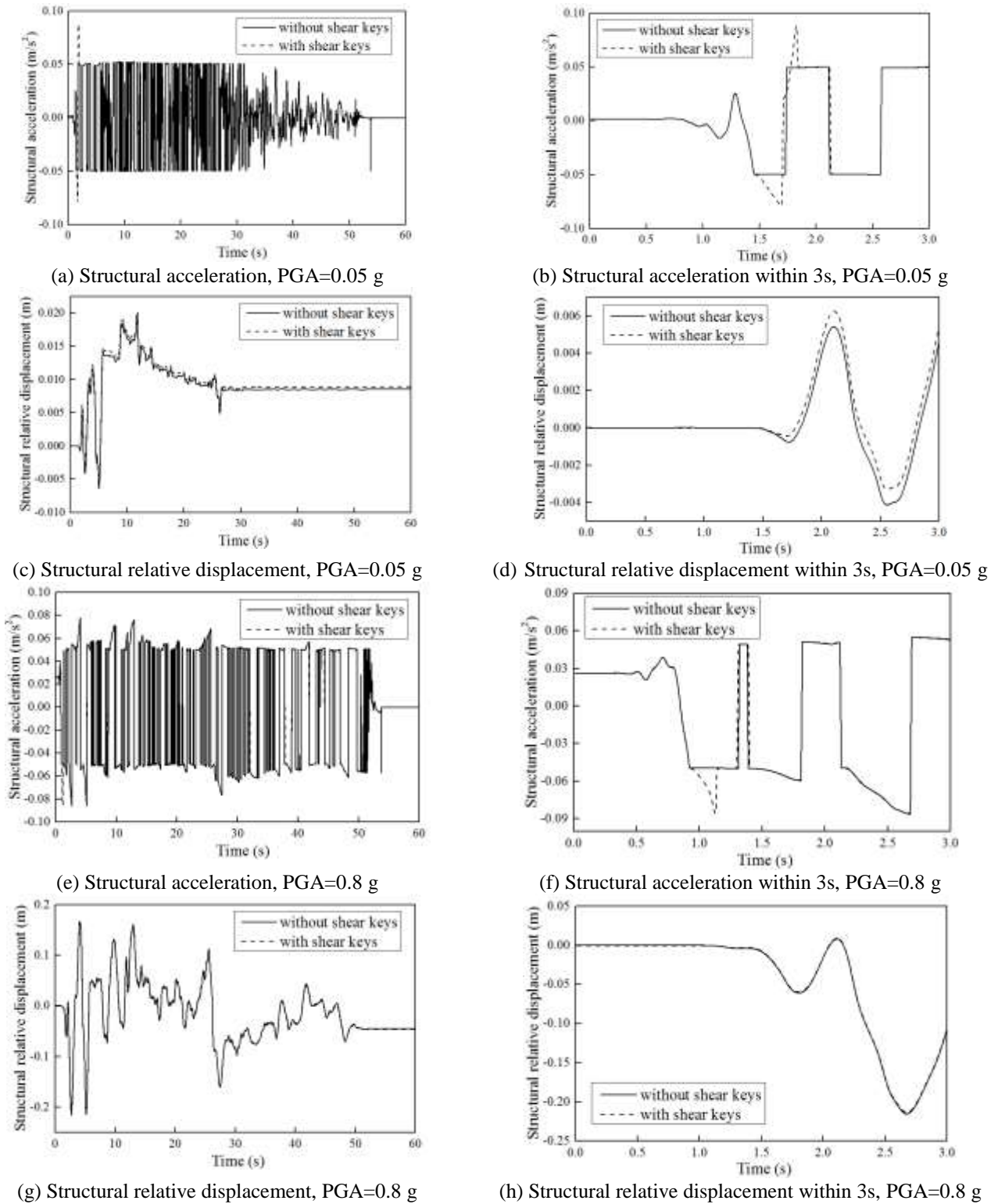
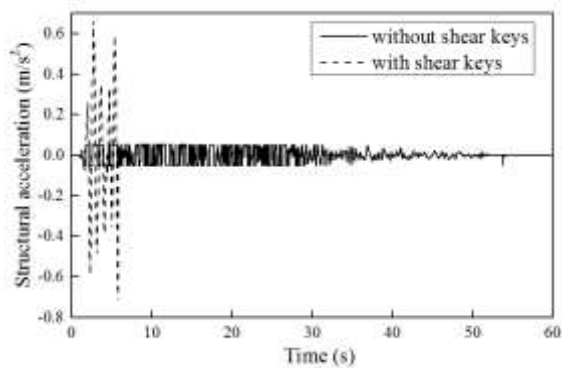


Fig. 3 Seismic responses for the case with $\mu_0=0.005$, $R=0.01 \text{ m}^{-1}$, $C=0 \text{ kN}\cdot\text{s}/\text{m}$, $K=100 \text{ kN}/\text{m}$, $h_1 = 1.0 \text{ m}$, $h_0 = 0.8 \text{ m}$, $F_k=20000 \text{ kN}/\text{m}$, $F_k=10 \text{ kN}$ under the first ground motion

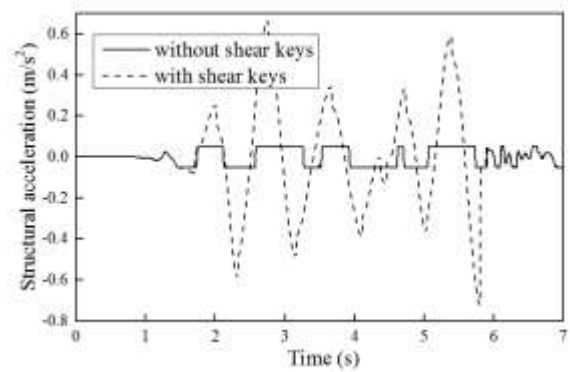
Finally, the seismic response demands of 99000000 cases were obtained and compared with the seismic capacities in Table 1. Only the general results are discussed in this section, although a lot of seismic responses and vulnerability curves are obtained.

6.1 Cases without a viscous damper

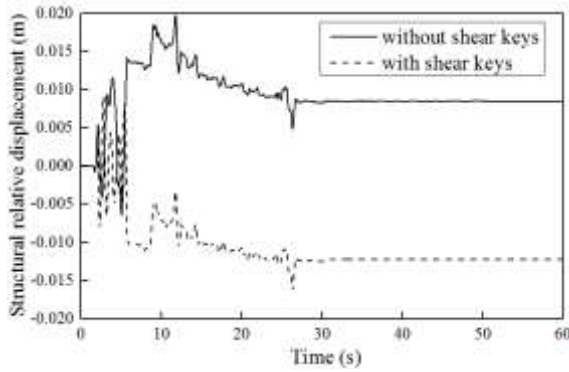
The seismic responses of the case with $\mu_0=0.005$, $R=0.01 \text{ m}^{-1}$, $C=0 \text{ kN}\cdot\text{s}/\text{m}$, $K=100 \text{ kN}/\text{m}$, $h_1 = 1.0 \text{ m}$ and $h_0 = 0.8$ are shown in Fig. 3, including the results without



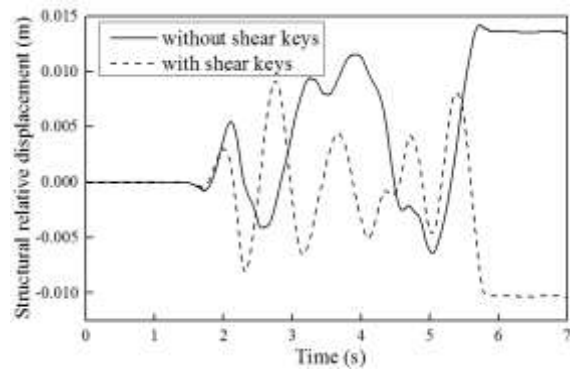
(a) Structural acceleration, PGA=0.05 g



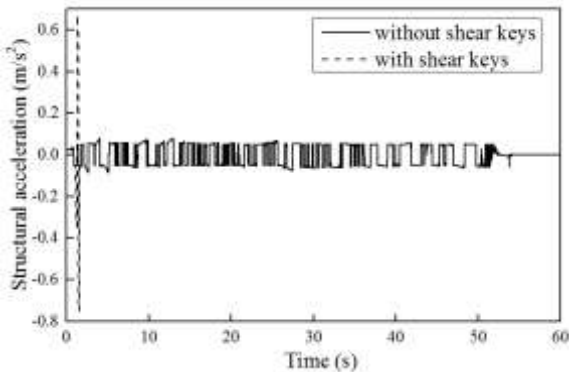
(b) Structural acceleration within 7s, PGA=0.05g



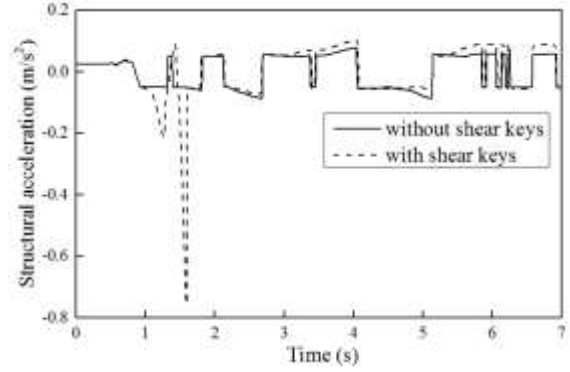
(c) Structural relative displacement, PGA=0.05 g



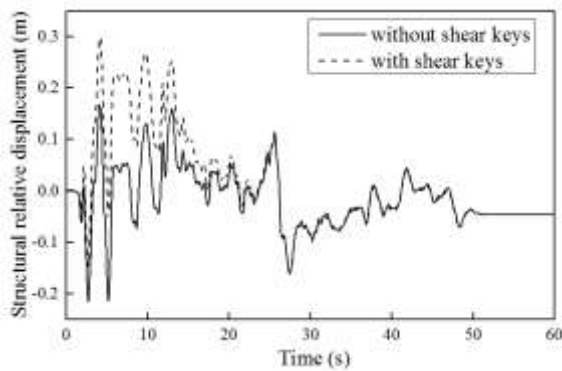
(d) Structural relative displacement within 7s, PGA=0.05 g



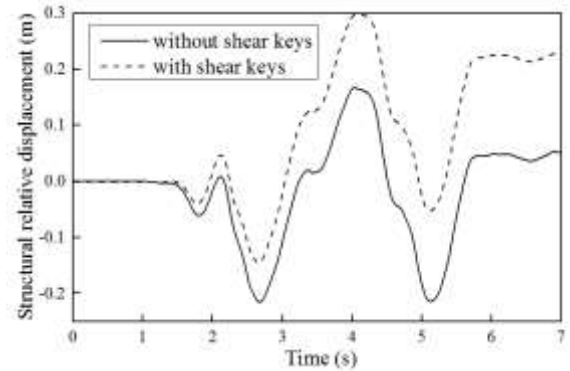
(e) Structural acceleration, PGA=0.8 g



(f) Structural acceleration within 7s, PGA=0.8 g



(g) Structural relative displacement, PGA=0.8 g



(h) Structural relative displacement within 7s, PGA=0.8 g

Fig. 4 Seismic responses for the case with $\mu_0=0.005$, $R=0.01 \text{ m}^{-1}$, $C=0 \text{ kN}\cdot\text{s}/\text{m}$, $K=100 \text{ kN}/\text{m}$, $h_1 = 1.0 \text{ m}$, $h_0 = 0.8 \text{ m}$, $K_k=20000 \text{ kN}/\text{m}$, $F_k=200 \text{ kN}$ under the first ground motion

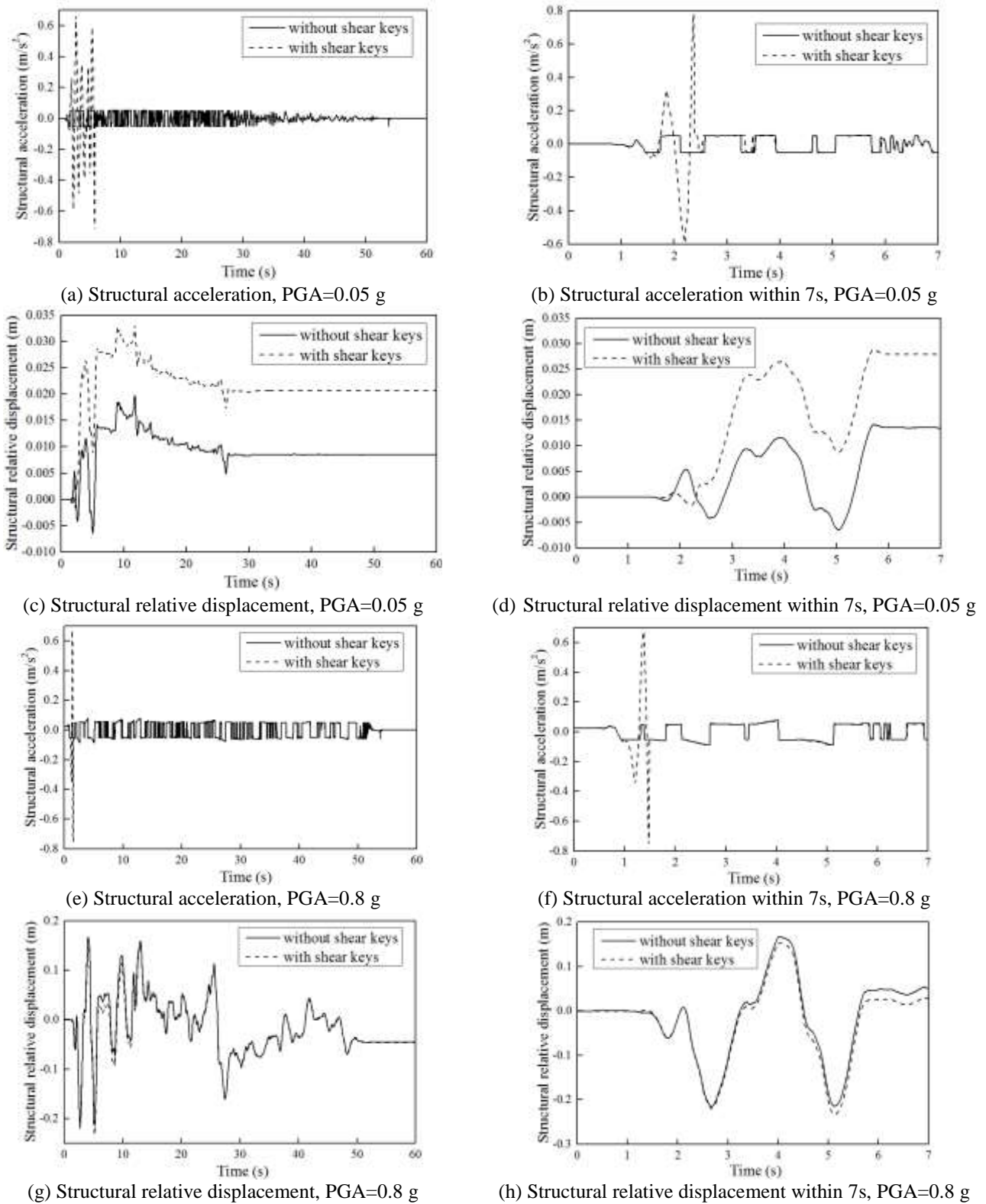
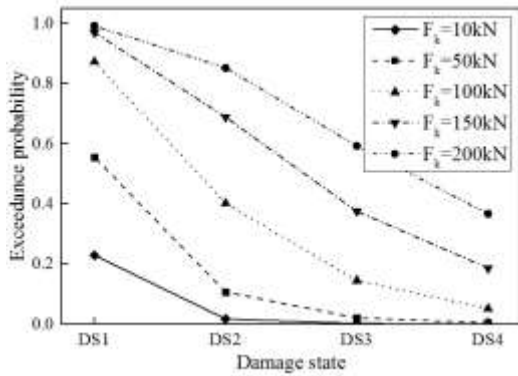


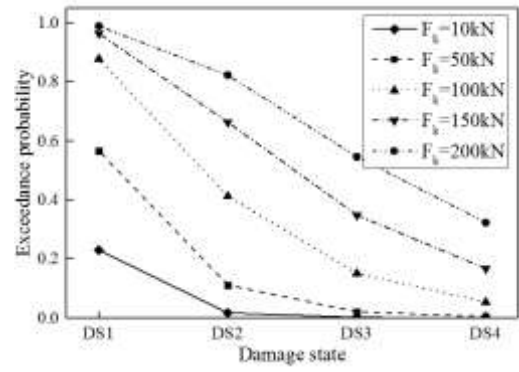
Fig. 5 Seismic responses for the case with $\mu_0=0.005$, $R=0.01 \text{ m}^{-1}$, $C=0 \text{ kN}\cdot\text{s}/\text{m}$, $K=100 \text{ kN}/\text{m}$, $h_1 = 1.0 \text{ m}$, $h_0 = 0.8 \text{ m}$, $K_k=100000 \text{ kN}/\text{m}$, $F_k=200 \text{ kN}$ under the first ground motion

any shear key and the results with the shear keys adopting $K_k=20000 \text{ kN}/\text{m}$ and $F_k=10 \text{ kN}$. Those shear keys can be easily destroyed by a small structural acceleration of $10/300=0.0333 \text{ m}/\text{s}^2$ when ignoring the disturbances of

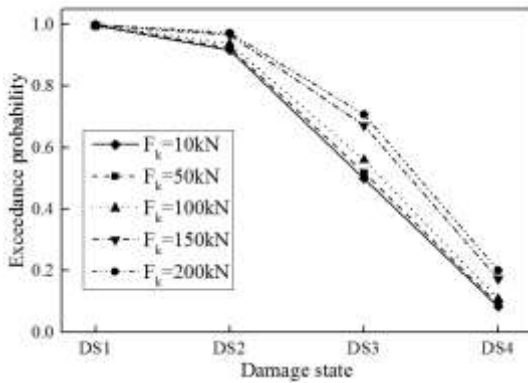
friction and spring actions. And in theory, the structural seismic responses with such feeble shear keys would be almost the same as those without any shear key.



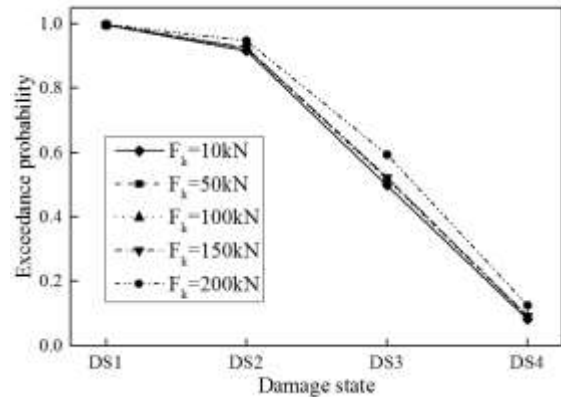
(a) Structural acceleration with $K_k=20000$ kN/m



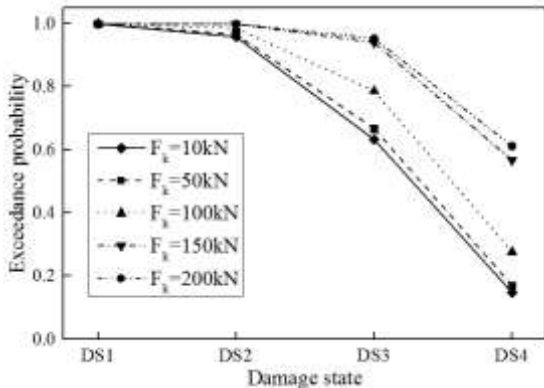
(b) Structural acceleration with $K_k=100000$ kN/m



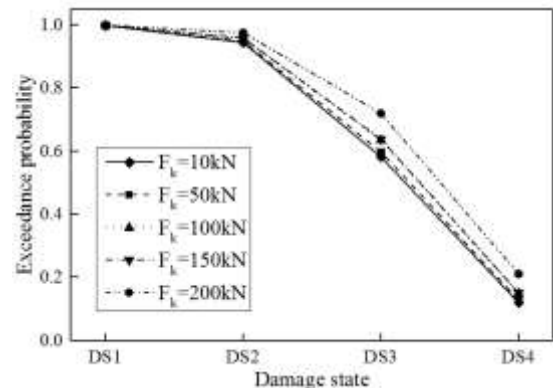
(c) Structural relative displacement with $K_k=20000$ kN/m



(d) Structural relative displacement with $K_k=100000$ kN/m



(e) Structural residual displacement with $K_k=20000$ kN/m



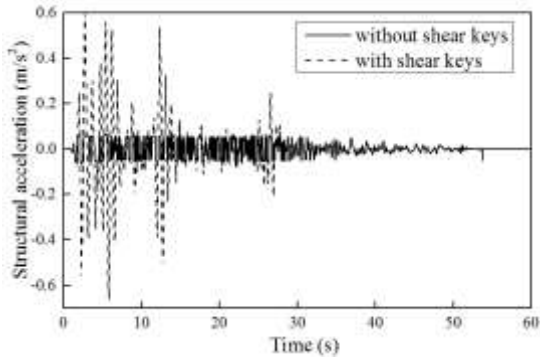
(f) Structural residual displacement with $K_k=100000$ kN/m

Fig. 6 The probabilities exceeding each damage state in Table 1 for the cases with $\mu_0=0.005$, $R=0.01$ m⁻¹, $C=0$ kN·s/m, $K=100$ kN/m, $h_1 = 1.0$ m, $h_0 = 0.8$ m and $PGA=0.8$ g by changing the cutting off force of shear keys

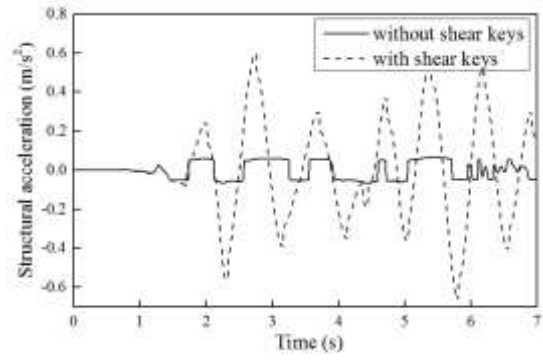
Figs. 3(a)-3(d) validate that those shear keys are cut off at the time of 1.8s and there is a little difference between the results with and without such feeble shear keys when subjected to an earthquake with $PGA=0.05$ g. This little difference is further reduced when PGA is increased from 0.05 g to 0.8 g as shown in Figs. 3(e)-3(h), and the cutting off time of shear keys is shortened from 1.8s to 1.1s.

When the cutting off force of shear keys increases from $F_k=10$ kN in Fig. 3 to $F_k=200$ kN in Fig. 4, the structural seismic responses with shear keys become more different from those without shear keys. When subjected to an earthquake with $PGA=0.05$ g in Figs. 4(a)-4(d), the structural peak acceleration is less than $0.1m/s^2$ since PGA

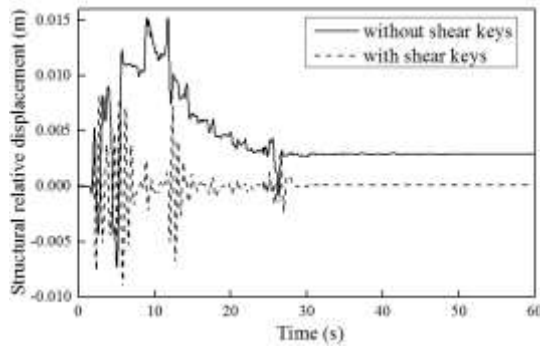
is so small for the case without any shear key, while this peak value is increased to be more than $200/300=0.666$ m/s² for the case with such strong shear keys. The cutting off time of shear keys is lengthened from 1.8s in Fig. 3(b) to 5.8s in Fig. 4(b), and it causes more difference between the displacement responses of the cases with and without shear keys before the failure of shear keys in Figs.4(c) and 4(d). It further causes the more different starting points of subsequent displacement responses, and leads to the more different residual displacements between the cases with and without shear keys. Overall, the peak relative displacement of the case with shear keys is less than that without any shear key, while the residual displacements are on the



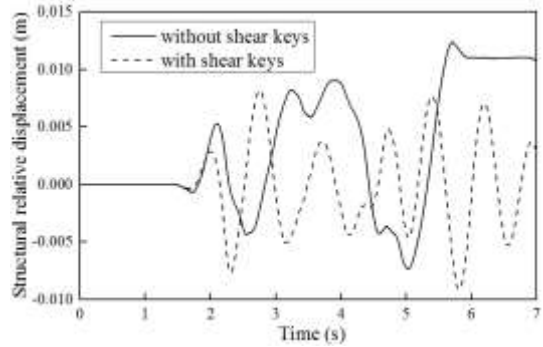
(a) Structural acceleration with $K_k=20000$ kN/m



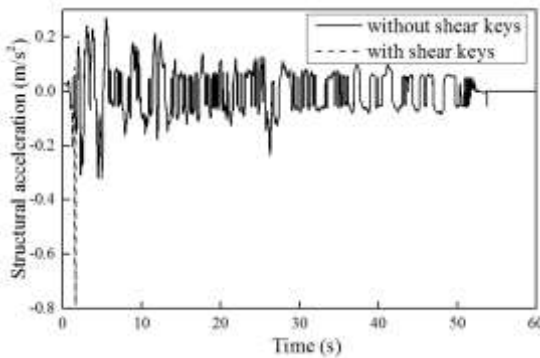
(b) Structural acceleration with $K_k=100000$ kN/m



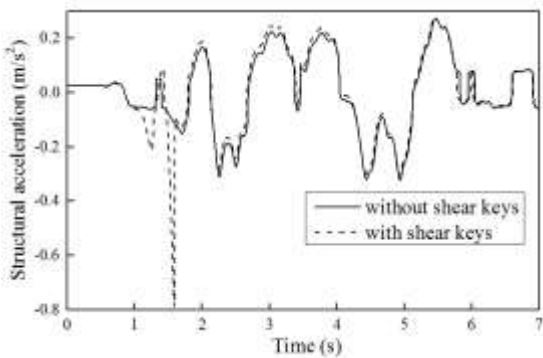
(c) Structural relative displacement with $K_k=20000$ kN/m



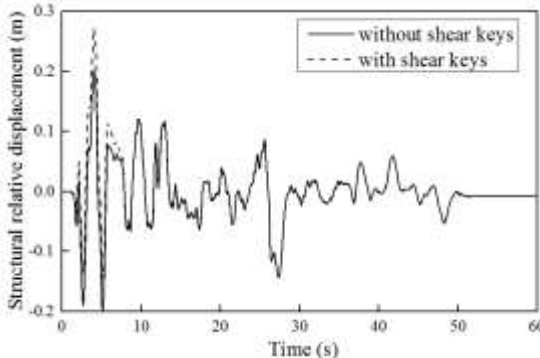
(d) Structural relative displacement with $K_k=100000$ kN/m



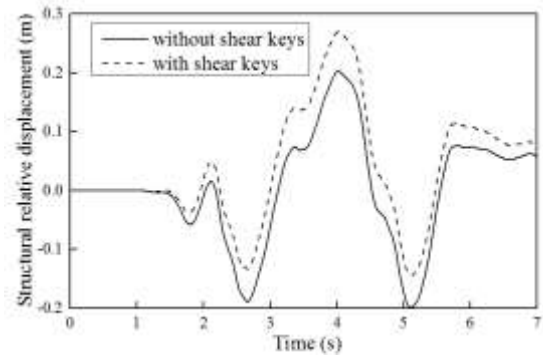
(e) Structural residual displacement with $K_k=20000$ kN/m



(f) Structural residual displacement with $K_k=100000$ kN/m



(g) Structural relative displacement, PGA=0.8 g



(h) Structural relative displacement within 7s, PGA=0.8 g

Fig. 7 Seismic responses for the case with $\mu_0=0.005$, $R=0.01$ m⁻¹, $C=100$ kN·s/m, $K=100$ kN/m, $h_1 = 1.0$ m, $h_0 = 0.1$ m, $K_k=20000$ kN/m, $F_k=200$ kN under the first ground motion

contrary. When PGA increases to PGA=0.8 g in Figs. 4(e)-4(h), the cutting off time of shear keys is moved forward to 1.6s. It reduces the difference between the displacement responses of the cases with and without shear keys before

the failure of shear keys and the difference of subsequent displacement responses. In this condition, however, the displacement responses of the case with shear keys are much larger than those without any shear key.

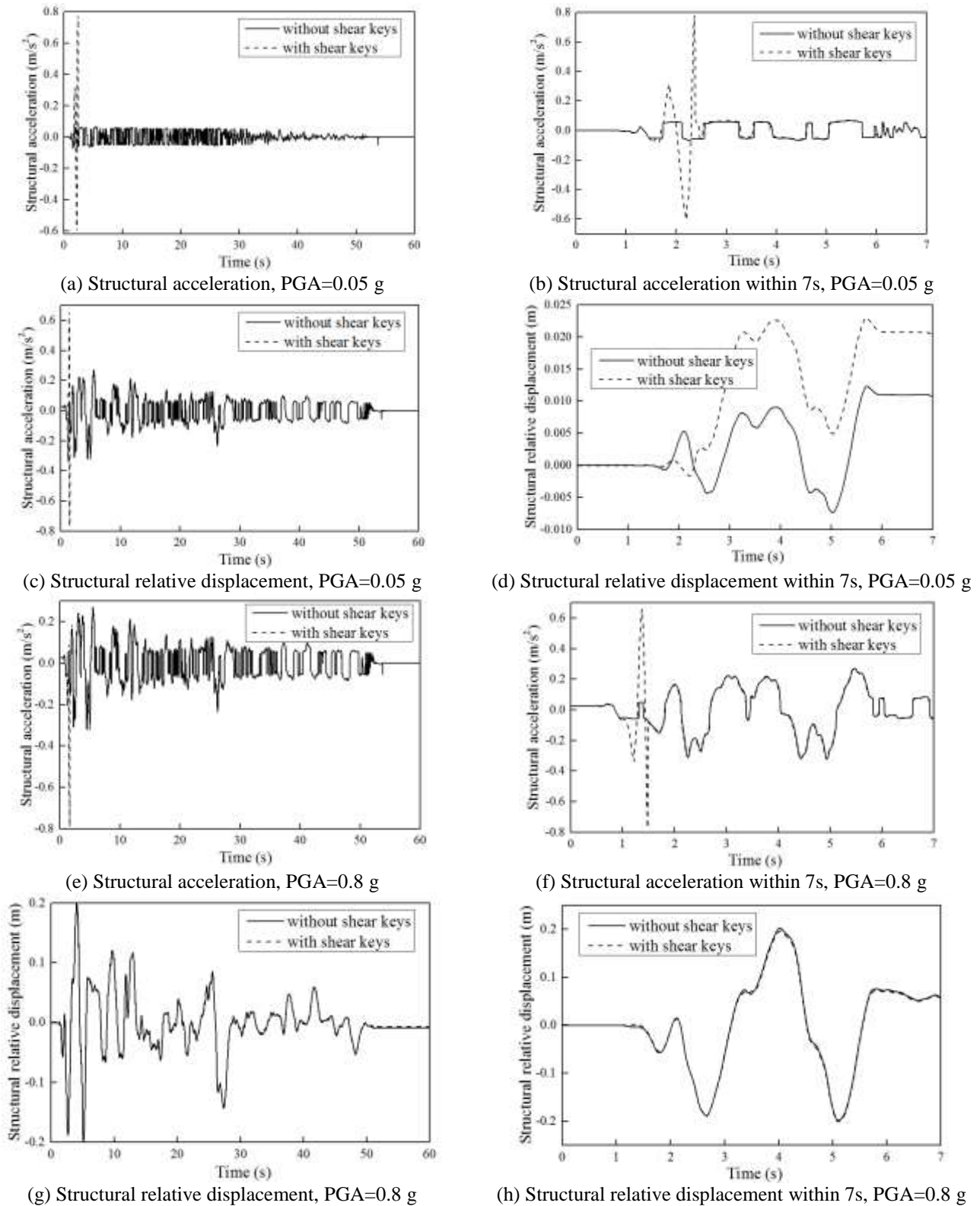
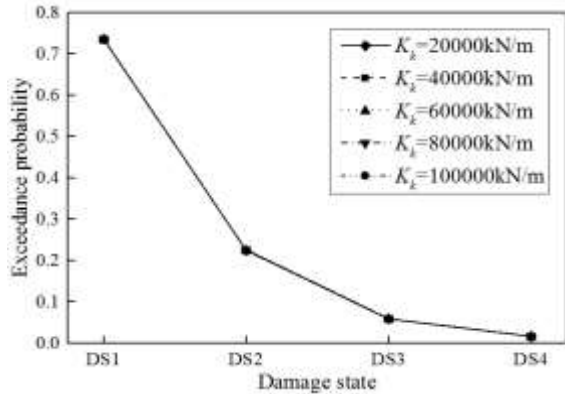


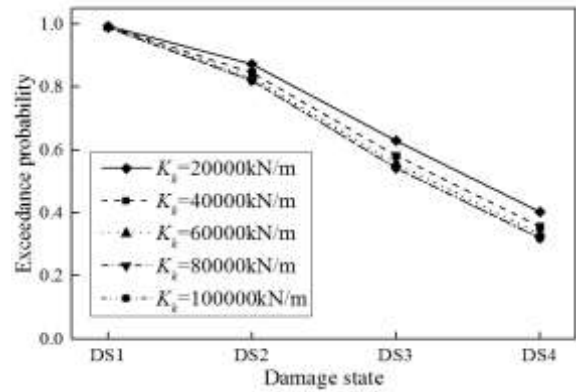
Fig. 8 Seismic responses for the case with $\mu_0=0.005$, $R=0.01 \text{ m}^{-1}$, $C=100 \text{ kN}\cdot\text{s}/\text{m}$, $K=100 \text{ kN}/\text{m}$, $h_1 = 1.0 \text{ m}$, $h_0 = 0.1 \text{ m}$, $K_k=100000 \text{ kN}/\text{m}$, $F_k=200 \text{ kN}$ under the first ground motion

When the spring constant of shear keys increases from $K_k=20000 \text{ kN}/\text{m}$ in Fig. 4 to $K_k=100000 \text{ kN}/\text{m}$ in Fig. 5, the difference between the seismic responses of the cases

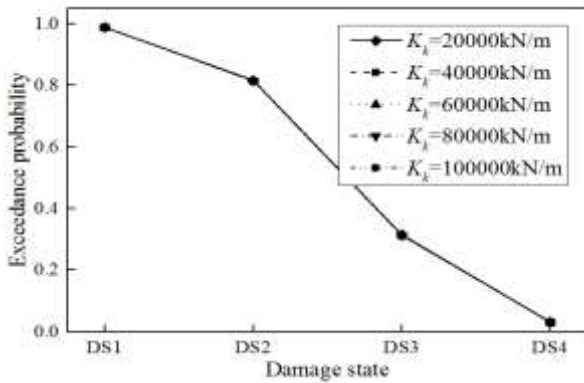
with and without shear keys in Fig. 5 is similar with that in Fig. 4, however, the different degree is reduced. For example, the cutting off time of shear keys is shortened



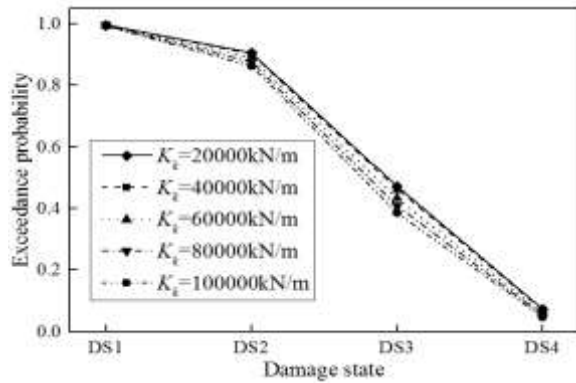
(a) Structural acceleration with $F_k=10$ kN



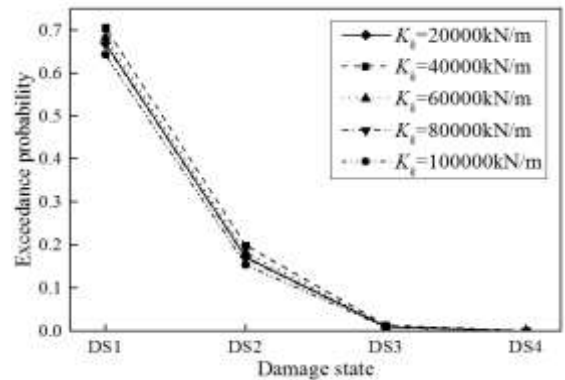
(b) Structural acceleration with $F_k=200$ kN



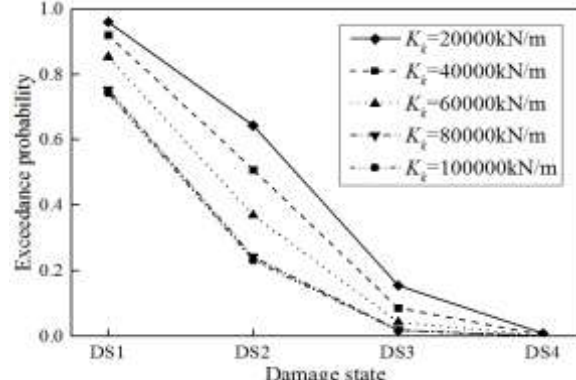
(c) Structural relative displacement with $F_k=10$ kN



(d) Structural relative displacement with $F_k=200$ kN



(e) Structural residual displacement with $F_k=10$ kN



(f) Structural residual displacement with $F_k=200$ kN

Fig. 9 The probabilities exceeding each damage state in Table 1 for the cases with $\mu_0=0.005$, $R=0.01$ m⁻¹, $C=100$ kN·s/m, $K=100$ kN/m, $h_1 = 1.0$ m, $h_0 = 0.1$ m and $PGA=0.8$ g by changing the spring constant of shear keys

from 5.8s in Fig. 4(b) to 2.3s in Fig. 5(b) when $PGA=0.05g$ and from 1.6s in Fig. 4(f) to 1.4s in Fig. 5(f) when $PGA=0.8$ g. It further reduces the difference between the displacement responses of the cases with and without shear keys before the failure of shear keys and the difference of subsequent displacement responses. When both the spring constant of shear keys and PGA are large enough, the displacement responses are almost the same between the cases with and without shear keys in Fig. 5(g).

As to further validate the above discussions, the probabilities, exceeding each damage state in Table 1, for the cases with $\mu_0=0.005$, $R=0.01$ m⁻¹, $C=0$ kN·s/m, $K=100$ kN/m, $h_1 = 1.0$ m, $h_0 = 0.8$ m and $PGA=0.8$ g are shown in Fig. 6. This figure validates that all of the seismic

responses increase with the cutting off force of shear keys. This rule is much more significant for the structural acceleration rather than for the structural relative and residual displacements. And this rule is more significant for the cases with $K_k=20000$ kN/m than for the cases with $K_k=100000$ kN/m. Fig. 6 also implies that all of the seismic responses decrease with the spring constant of shear keys, however, this rule is insignificant. Furthermore, this rule is more significant for the cases with $F_k=200$ kN than for the cases with $F_k=10$ kN.

6.2 Cases with a viscous damper

When the damping constant increases from $C=0$ kN·s/m

in Fig. 4 to $C=100$ kN·s/m in Fig. 7 and the length of spring with zero stress decreases from $h_0 = 0.8$ m in Fig. 4 to $h_0 = 0.1$ m in Fig. 7, the viscous damping action will disturb the cutting off of shear keys. When subjected to an earthquake with $PGA=0.05$ g in Figs. 7(a)-7(d), the structural peak acceleration is less than 0.1m/s^2 since PGA is so small for the case without any shear key. However, the structural peak acceleration 0.68m/s^2 in Figs. 7(a) and 7(b) is not able to cut off the shear keys since the shearing force of shear keys is less than the cutting off force of 200 kN due to the co-working of viscous damper. The structure with the shear keys is un-isolated in essence, and its acceleration response is much larger than that without the shear keys in Figs. 7(a) and 7(b) while its relative and residual displacement responses are much less than those without the shear keys in Figs. 7(c) and 7(d). When PGA increases to $PGA=0.8$ g in Figs. 7(e)-7(h), a structural peak acceleration 0.8 m/s^2 , being larger than $200/300=0.666\text{ m/s}^2$, cuts off the shear keys at the time of 1.6s. It reduces the difference between the seismic responses of the cases with and without shear keys. However, the acceleration and displacement responses of the case with shear keys are still larger than those without any shear key.

When the spring constant of shear keys increases from $K_k=20000$ kN/m in Fig. 7 to $K_k=100000$ kN/m in Fig. 8, the difference between the seismic responses of the cases with and without shear keys in Fig. 8 is reduced when compared with that in Fig. 7. For example, the shear keys are cut off at the time of 2.3s in Figs. 8(a) and 8(b) instead of being well in Figs. 7(a) and 7(b) when $PGA=0.05$ g, because the increase of the spring constant of shear keys increases the ratio of shear key force to the viscous damping force. It reduces the difference between the displacement responses of the cases with and without shear keys before the failure of shear keys and the difference of subsequent displacement responses. When both the spring constant of shear keys and PGA are large enough in Figs. 8(e) and 8(f), the displacement responses with shear keys are almost the same as those without any shear key in Fig. 8(g).

As to further validate the above discussions, the probabilities, exceeding each damage state in Table 1, for the cases with $\mu_0=0.005$, $R=0.01\text{ m}^{-1}$, $C=100$ kN·s/m, $K=100$ kN/m, $h_1 = 1.0$ m, $h_0 = 0.1$ m and $PGA=0.8$ g are shown in Fig. 9. Fig. 9 shows that all of the seismic responses increase with the cutting off force of shear keys. This rule is much more significant for the structural acceleration rather than for the structural relative displacement and residual displacement. Fig. 9 also implies that all of the seismic responses decrease with the spring constant of shear keys. This rule is more significant for the cases with $F_k=200$ kN than for the cases with $F_k=10$ kN, especially for the structural residual displacement responses.

7. Further optimization of isolation system

Based on the above parameter analysis and discussion, the vertical spring-viscous damper-Coulomb friction isolation system has a lot of merits during earthquakes (Wei *et al.* 2019a), however, they can be further improved by

using the advanced technique in the friction region.

When the structural relative displacement $d_r = 0$, the horizontal component of spring force is 0 and the central friction force of concave friction distribution is so small that they only insignificantly disturb the cutting off of shear keys used for service loadings. As to further reduce the residual displacement response and the disturbance degree of the cutting off of shear keys, the central friction coefficient μ_0 of contact surface can be further reduced from $\mu_0=0.005$ to $\mu_0=0.001$ by using the superlubrication friction technique.

After the shear keys are cut off during earthquakes, the loose spring instead of the strong spring can be used to reduce the structural acceleration response. The increasing horizontal component of spring stiffness along with the structural relative displacement can avoid resonance and reduce the displacement response. Simultaneously, the friction force on the concave friction surface increases along with the structural relative displacement to increase the energy dissipation capacity, and thus to reduce the relative displacement response. Furthermore, the vertical force of spring can be controlled to avoid the structural interfacial detachment from the ground (Wei *et al.* 2018e), and is increased to increase the friction force when the relative displacement increases.

If the increment ratio R of concave friction distribution adopts a constant value such as $R=0.01\text{ m}^{-1}$, the friction force will be larger than the horizontal component of spring force within a certain relative displacement in Fig. 10(a), and thus the structural residual displacement is always large after earthquakes. If R is changed from a constant value to a variable value, the friction force can be controlled to be always less than the horizontal component of spring force within any relative displacement in Fig.10(b). Based on $F_{sh} = F_{fh}$ in Eqs. (3) and (9), such a variable R can be obtained as follows

$$R = \frac{K(\sqrt{h_1^2 + d_r^2} - h_0)(d_r - \mu_0 h_1) - \mu_0 m g \sqrt{h_1^2 + d_r^2}}{d_r[m g \sqrt{h_1^2 + d_r^2} + K(\sqrt{h_1^2 + d_r^2} - h_0)h_1]} \quad (10)$$

As to achieve $F_{sh} > F_{fh}$, the variable R can be obtained by

$$R = \frac{K(\sqrt{h_1^2 + d_r^2} - h_0)(d_r - \mu_0 h_1) - \mu_0 m g \sqrt{h_1^2 + d_r^2}}{d_r[m g \sqrt{h_1^2 + d_r^2} + K(\sqrt{h_1^2 + d_r^2} - h_0)h_1]} - V_d \quad (11)$$

The constant parameter V_d can adopt a small value, such as 0.001, 0.002 and 0.003 m^{-1} , to cause the difference between F_{sh} and F_{fh} .

The cutting off force of shear keys should be as small as possible to reduce the structural acceleration response, however, it should satisfy service loadings. Simultaneously, the spring constant of shear keys should be as large as possible to reduce the disturbance of spring, friction and viscous damping actions. The cutting off force and spring constant of shear keys temporarily adopt $F_k=50$ kN and $K_k=100000$ kN/m in this section. When those parameters of shear keys and the parameters in Fig. 10(b) are used, the probabilities of the structural peak acceleration and peak relative displacement, exceeding different damage states in Table 1, are shown in Figures 11 and 12, respectively. If a

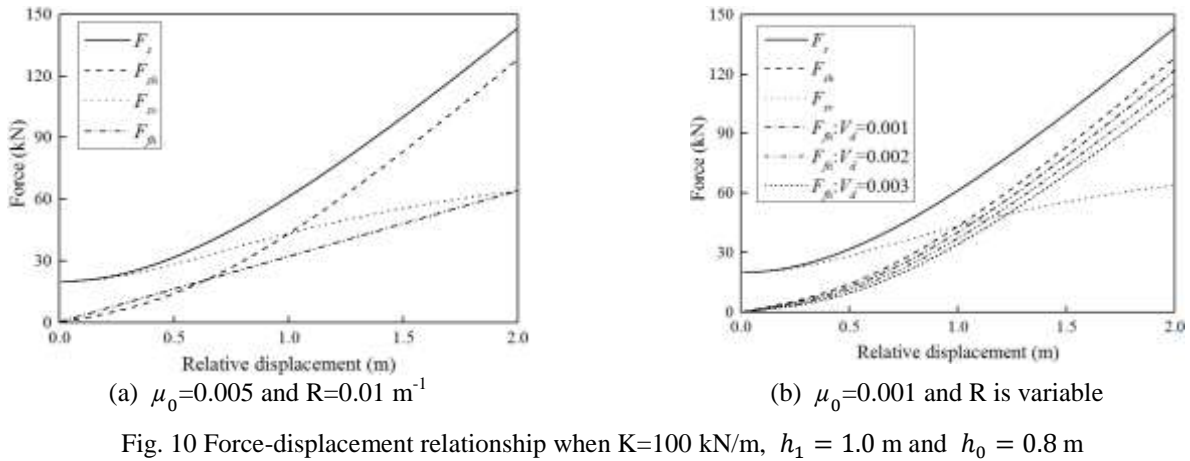


Fig. 10 Force-displacement relationship when $K=100 \text{ kN/m}$, $h_1 = 1.0 \text{ m}$ and $h_0 = 0.8 \text{ m}$

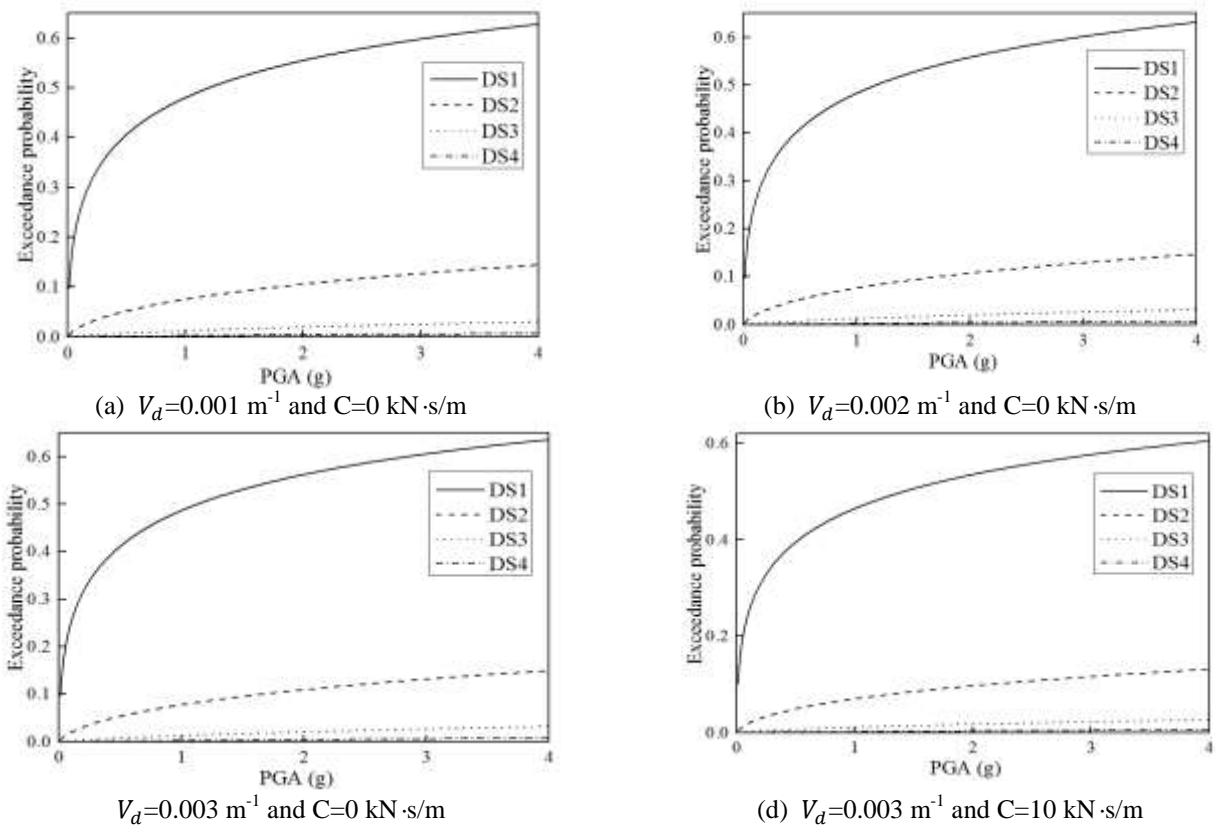


Fig. 11 Structural peak acceleration when $\mu_0=0.001$, $K=100 \text{ kN/m}$, $h_1 = 1.0 \text{ m}$ and $h_0 = 0.8 \text{ m}$

viscous damper with a small damping constant $C=10\text{kN}\cdot\text{s/m}$ is added to the case with $\mu_0=0.001$, $V_d=0.003 \text{ m}^{-1}$, $K=100 \text{ kN/m}$, $h_1 = 1.0 \text{ m}$ and $h_0 = 0.8 \text{ m}$, the corresponding results are shown in Figs. 11(d) and 12(d). Furthermore, the exceedance probabilities of structural residual displacement are almost 0 due to $F_{sh} > F_{fh}$, and are not listed here.

The exceedance probabilities of the structural peak acceleration and peak relative displacement increase with PGA in Figs. 11 and 12. When $V_d=0.001, 0.002, 0.003 \text{ m}^{-1}$, $C=0 \text{ kN}\cdot\text{s/m}$ and $V_d=0.003 \text{ m}^{-1}$, $C=10 \text{ kN}\cdot\text{s/m}$ under the earthquakes with $\text{PGA}=0.8 \text{ g}$, the probabilities of the

structural peak acceleration, exceeding DS1 in Table 1, are 45.6%, 45.9%, 46.2% and 44.2%, respectively. The corresponding probabilities of the structural peak relative displacement, exceeding DS3 in Table 1, are 39.5%, 40.5%, 41.4% and 38.2%, respectively. All of those exceedance probabilities increase when V_d increases, which indicates that a decrease of friction force reduces the dissipation efficiency of earthquake energy. The adding of the viscous damper with a small damping constant $C=10 \text{ kN}\cdot\text{s/m}$ can decrease the structural peak relative displacement, and peak acceleration, which implies that the viscous damping action can dissipate the earthquake energy as well as the friction

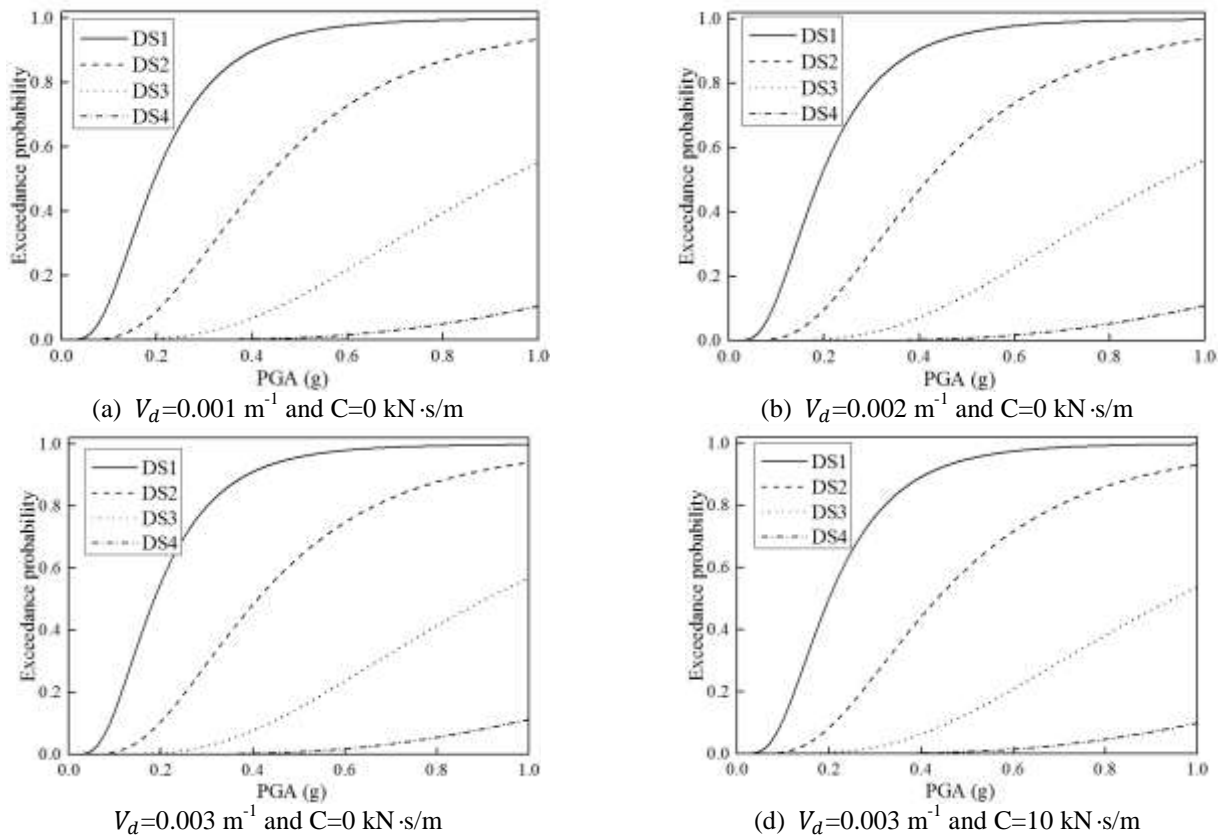


Fig. 11 Structural peak acceleration when $\mu_0=0.001$, $K=100 \text{ kN/m}$, $h_1 = 1.0 \text{ m}$ and $h_0 = 0.8 \text{ m}$

action, however, the installation and maintenance of viscous damper increases the cost of isolation system. All of the above exceedance probabilities are much less than the results of the similar cases in the previous sections. Importantly, the isolation system in this section doesn't need repair except the installation of new shear keys after earthquakes since the structural residual displacement is almost 0.

8. Conclusions

This paper investigates the influence of shear keys on the seismic performance of a vertical spring-viscous damper-concave Coulomb friction isolation system. The main conclusions are drawn as follows:

- (1) The shear keys are set in a seismic isolation system to resist the long-term service loadings, and are cut off to isolate the earthquakes. The cutting off process of shear keys should be simulated in a numerical analysis to accurately predict the seismic responses of isolation system.
- (2) Ignoring the cutting off process of shear keys usually leads to untrue seismic responses in a numerical analysis, and many of them are unsafe to design an isolated structure. And those errors will be increased by increasing the cutting off force of shear keys and decreasing the spring constant of shear keys, especially under a feeble earthquake.
- (3) The friction action, the spring action and the viscous damping action will disturb the cutting off process of shear

keys. For example, the viscous damping action postpones the cutting off time of shear keys during earthquakes, and reduces the seismic isolation efficiency. However, this point can be improved by increasing the spring constant of shear keys.

Acknowledgements

This research is jointly supported by the National Natural Science Foundations of China under grant No. 51778635 and 51778630, the Natural Science Foundations of Hunan Province under grant No.2019JJ40386, the Research Program on Displacement Limitation Technology of Half-through Railway Arch Bridge under grant No.science2018-81 and the Science and Technology Project of Sichuan Province under grant No.2019YFG0048. The above support is greatly appreciated.

References

- Antonyuk, E.Y. and Plakhtienko, N.P. (2004), "Dynamic modes of one seismic-damping mechanism with frictional bonds", *Int. Appl. Mech.*, **40**(6), 702-708. <https://doi.org/10.1023/B:INAM.0000041399.99257.b3>.
- Begley, C.J. and Virgin, L.N. (1998), "Impact response and the influence of friction", *J. Sound Vib.*, **211**(5), 801-818. <https://doi.org/10.1006/jsvi.1997.1389>.
- Chung, L.L., Kao, P.S., Yang, C.Y., Wu, L.Y. and Chen, H.M.

- (2015), "Optimal frictional coefficient of structural isolation system", *J. Vib. Control*, **21**(3), 525-538. <https://doi.org/10.1177/1077546313487938>.
- Cui, S. (2012), "Integrated design methodology for isolated floor systems in single-degree-of-freedom structural fuse systems", Ph.D. Dissertation, State University of New York, Buffalo.
- Fahjan, Y. and Ozdemir, Z. (2008), "Scaling of earthquake accelerograms for non-linear dynamic analysis to match the earthquake design spectra", *Proceedings of the 14th World Conference on Earthquake Engineering*, Chinese Society for Earthquake Engineering, Beijing, China.
- Flom, D.G. and Bueche, A.M. (1959), "Theory of rolling friction for spheres", *J. Appl. Phys.*, **30**(11), 1725-1730.
- Guerreiro, L., Azevedo, J. and Muhr, A.H. (2007), "Seismic tests and numerical modeling of a rolling-ball isolation system", *J. Earthq. Eng.*, **11**(1), 49-66. <https://doi.org/10.1080/13632460601123172>.
- Harvey, P.S. and Gavin, H.P. (2013), "The nonholonomic and chaotic nature of a rolling isolation system", *J. Sound Vib.*, **332**(14), 3535-3551. <https://doi.org/10.1016/j.jsv.2013.01.036>.
- Harvey, P.S. and Gavin, H.P. (2014), "Double rolling isolation systems: a mathematical model and experimental validation", *Int. J. Nonlinear Mech.*, **61**(1), 80-92. <https://doi.org/10.1016/j.ijnonlinmec.2014.01.011>.
- Harvey, P.S. and Gavin, H.P. (2015), "Assessment of a rolling isolation system using reduced order structural models", *Eng. Struct.*, **99**, 708-725. <https://doi.org/10.1016/j.engstruct.2015.05.022>.
- Harvey, P.S., Wiebe, R. and Gavin, H.P. (2013), "On the chaotic response of a nonlinear rolling isolation system", *Physica D: Nonlinear Phenomena*, **256-257**, 36-42. <https://doi.org/10.1016/j.physd.2013.04.013>.
- Harvey, P.S., Zehil, G.P. and Gavin, H.P. (2014), "Experimental validation of a simplified model for rolling isolation systems", *Earthq. Eng. Struct. D.*, **43**(7), 1067-1088. <https://doi.org/10.1002/eqe.2387>.
- Ismail, M. (2015), "An isolation system for limited seismic gaps in near-fault zones", *Earthq. Eng. Struct. D.*, **44**(7), 1115-1137. <https://doi.org/10.1002/eqe.2504>.
- Ismail, M. and Casas, J.R. (2014), "Novel isolation device for protection of cable-stayed bridges against near-fault earthquakes", *J. Bridge Eng.*, **19**(8), 50-65. [https://doi.org/10.1061/\(ASCE\)BE.1943-5592.0000509](https://doi.org/10.1061/(ASCE)BE.1943-5592.0000509).
- Ismail, M., Rodellar, J. and Pozo, F. (2014), "An isolation device for near-fault ground motions", *Struct. Control Health Monit.*, **21**(3), 249-268. <https://doi.org/10.1002/stc.1549>.
- Ismail, M., Rodellar, J. and Pozo, F. (2015), "Passive and hybrid mitigation of potential near-fault inner pounding of a self-braking seismic isolator", *Soil Dynam. Earthq. Eng.*, **69**(2), 233-250. <https://doi.org/10.1016/j.soildyn.2014.10.019>.
- Jangid, R.S. (2000), "Stochastic seismic response of structures isolated by rolling rods", *Eng. Struct.*, **22**(8), 937-946. [https://doi.org/10.1016/S0141-0296\(99\)00041-3](https://doi.org/10.1016/S0141-0296(99)00041-3).
- Jangid, R.S. and Londhe, Y.B. (1998), "Effectiveness of elliptical rolling rods for base isolation", *J. Struct. Eng.*, **124**(4), 469-472. [https://doi.org/10.1061/\(ASCE\)0733-9445\(1998\)124:4\(469\)](https://doi.org/10.1061/(ASCE)0733-9445(1998)124:4(469)).
- JTJ004-89, Standard of the Ministry of Communications of P.R. China (1989), Specifications of Earthquake Resistant Design for Highway Engineering, China Communications Press, Beijing, China (in Chinese).
- Kosantantinidis, D. and Makris, N. (2009), "Experimental and analytical studies on the response of freestanding laboratory equipment to earthquake shaking", *Earthq. Eng. Struct. D.*, **38**(6), 827-848. <https://doi.org/10.1002/eqe.871>.
- Kurita, K., Aoki, S., Nakanishi, Y., Tominaga, K. and Kanazawa, M. (2011), "Fundamental characteristics of reduction system for seismic response using friction force", *J. Civil Eng. Architect.*, **5**(11), 1042-1047.
- Lee, G.C., Ou, Y.C., Niu, T.C., Song, J.W. and Liang, Z. (2010), "Characterization of a roller seismic isolation bearing with supplemental energy dissipation for highway bridges", *J. Struct. Eng.*, **136**(5), 502-510. [https://doi.org/10.1061/\(ASCE\)ST.1943-541X.0000136](https://doi.org/10.1061/(ASCE)ST.1943-541X.0000136).
- Lewis, A.D. and Murray, R.M. (1995), "Variational principles for constrained systems: Theory and experiment", *Int. J. Nonlinear Mech.*, **30**(6), 793-815.
- Nanda, R.P., Agarwal, P. and Shrikhande, M. (2012), "Base isolation system suitable for masonry buildings", *Asian J. Civil Eng. (Building and Housing)*, **13**(2), 195-202.
- Ortiz, N.A., Magluta, C. and Roitman, N. (2015), "Numerical and experimental studies of a building with roller seismic isolation bearings", *Struct. Eng. Mech.*, **54**(3), 475-489. <http://dx.doi.org/10.12989/sem.2015.54.3.475>.
- Ou, Y.C., Song, J.W. and Lee, G.C. (2010), "A parametric study of seismic behavior of roller seismic isolation bearings for highway bridges", *Earthq. Eng. Struct. D.*, **39**(5), 541-559. <https://doi.org/10.1002/eqe.958>.
- Siringoringo, D.M. and Fujino, Y. (2015), "Seismic response analyses of an asymmetric base-isolated building during the 2011 Great East Japan (Tohoku) Earthquake", *Struct. Control Health Monit.*, **22**(1), 71-90. <https://doi.org/10.1002/stc.1661>.
- Tsai, C.S., Lin, Y.C., Chen, W.S. and Su, H.C. (2010), "Tri-directional shaking table tests of vibration sensitive equipment with static dynamics interchangeable-ball pendulum system", *Earthq. Eng. Eng. Vib.*, **9**(1), 103-112. <https://doi.org/10.1007/s11803-010-9009-4>.
- Wang, S.J., Hwang, J.S., Chang, K.C., Shiau, C.Y., Lin, W.C., Tsai, M.S., Hong, J.X. and Yang, Y.H. (2014), "Sloped multi-roller isolation devices for seismic protection of equipment and facilities", *Earthq. Eng. Struct. D.*, **43**(10), 1443-1461. <https://doi.org/10.1002/eqe.2404>.
- Wang, Y.J., Wei, Q.C., Shi, J. and Long, X.Y. (2010), "Resonance characteristics of two-span continuous beam under moving high speed trains", *Latin Am. J. Solids Struct.*, **7**(2), 185-199. <http://dx.doi.org/10.1590/S1679-78252010000200005>.
- Wei, B., Wang, P., He X.H. and Jiang, L.Z. (2018), "Seismic isolation characteristics of a friction system", *J. Test. Eval.*, **46**(4), 1411-1420. DOI: 10.1520/JTE20160598.
- Wei, B., Wang, P., He, X.H. and Jiang, L.Z. (2018), "The impact of the convex friction distribution on the seismic response of a spring-friction isolation system", *KSCSE J. Civil Eng.*, **22**(4), 1203-1213. <https://doi.org/10.1007/s12205-017-0938-6>.
- Wei, B., Yang, T. H., Jiang, L.Z. and He, X.H. (2018), "Effects of uncertain characteristic periods of ground motions on seismic vulnerabilities of a continuous track-bridge system of high-speed railway", *Bull. Earthq. Eng.*, **16**(9), 3739-3769. <https://doi.org/10.1007/s10518-018-0326-8>.
- Wei, B., Yang, T. H., Jiang, L.Z. and He, X.H. (2018), "Effects of friction-based fixed bearings on the seismic vulnerability of a high-speed railway continuous bridge", *Adv. Struct. Eng.*, **21**(5), 643-657. <https://doi.org/10.1177/1369433217726894>.
- Wei, B., Zhuo, Y., Li, C.B. and Yang, M.G. (2019), "Parameter optimization of a vertical spring-viscous damper-Coulomb friction system", *J. Shock Vib.*, doi: 10.1155/2019/5764946.
- Wei, B., Zuo, C.J., He, X.H. and Hu, Q.Y. (2019), "Earthquake isolation of a spring-damper-friction system with a convex friction distribution", *J. Test. Eval.*, **2019**, doi:10.1520/JTE20170275.
- Wei, B., Zuo, C.J., He, X.H., Jiang, L.Z. and Wang T. (2018), "Effects of vertical ground motions on seismic vulnerabilities of a continuous track-bridge system of high-speed railway", *Soil Dynam. Earthq. Eng.*, **115**, 281-290. <https://doi.org/10.1016/j.soildyn.2018.08.022>.
- Yim, C.S., Chopra, A.K. and Penzien, J. (1980), "Rocking

response of rigid blocks to earthquakes”, *Earthq. Eng. Struct. D.*, **8**(6), 565-587. <https://doi.org/10.1002/eqe.4290080606>.

CC